increased to the extent that above pH 9, the dimethylated complex, which cannot lose its positive charge, loses its Ga(III) in favor of the deprotonated form of Ga(III)-PLED.

It has been shown that the In(III) ion has a preference for carboxylate donors over phenolate or hydroxypyridine donor groups.[13] Thus the stability constant of the DTPA-In(III) complex is greater than those of PLED and DMPLED. Since the summation of the log protonation constants of the latter, even that of DMPLED, is larger than the basicity sum of DTPA, there is no need to make comparisons of the In(III) chelates of these ligands with species distribution curves: a 1:1:1 system of In(III), DMPLED, and DTPA would show only DTPA complexes, and those of DMPLED would not appear at all. In other words there is no competition in this system.

Influence of Charge and Stability of the Complexes on Biodistribution. It is shown in a separate report[11] that although the trivalent metal complexes of HBPLED, Me_4HBPLED and DMPLED have different overall charges (-1, 0, and +1), the biodistributions of the metal complexes in rats are similar and all complexes undergo renal clearance. The ^{111}In and ^{68}Ga complexes resemble the biodistribution and clearance route of the complexes of the parent ligands HBED and PLED. Thus it seems that biodistributions of these complexes are dependent on other factors, which are more important in controlling behavior, than the charge on the complex molecule. It is suggested that the zwitterions in formulas **5** and **6** and corresponding dipolar functional groups in their metal complexes are highly solvated in aqueous solution. This makes both ligands and metal complexes highly hydrophilic and accounts for the observed biodistributions and clearance routes.

When examining a similar complex EHPG (ethylenebis((hydroxyphenyl)glycine),[20] we have found very different in vivo behavior between the iron, indium and gallium complexes. This is not the case for the complexes of HBPLED, Me_4HBPLED, and DMPLED where very similar biodistribution patterns were obtained with indium and gallium and for DMPLED (the only ligand studied) with iron. The similarity in biodistribution is presumably due to the similar pM values of all the complexes and the fact that they are all greater than the corresponding pM value for the metal transferrin complex.

Acknowledgment. This work was supported by NIH Grant CA-42925.

(20) Madsen, S. L.; Bannochie, C. J.; Martell, A. E.; Mathias, C. J.; Welch, M. J. *J. Nucl. Med.* **1990**, *31*, 1662.

Contribution from the Evans Laboratory of Chemistry, The Ohio State University, 120 West 18th Avenue, Columbus, Ohio 43210

Metallobiochemistry of Magnesium. Coordination Complexes with Biological Substrates: Site Specificity, Kinetics and Thermodynamics of Binding, and Implications for Activity†

J. A. Cowan

Received August 29, 1990

The association constant (K_a), activation free energy (ΔG^*), and off-rate for magnesium binding (k_{off}) to glucose 1-phosphate (K_a = 15 M^{-1}, ΔG^* = 12.7 kcal mol^{-1}, k_{off} = 2.9 × 10^3 s^{-1}), glucose 6-phosphate (K_a = 8 M^{-1}, ΔG^* = 12.7 kcal mol^{-1}, k_{off} = 3.1 × 10^3 s^{-1}), acetyl phosphate (K_a = 9 M^{-1}, ΔG^* = 13.1 kcal mol^{-1}, k_{off} = 1.5 × 10^3 s^{-1}), AMP^{2-} (K_a = 18 M^{-1}, ΔG^* = 12.7 kcal mol^{-1}, k_{off} = 3.4 × 10^3 s^{-1}), ADP^{3-} (K_a = 2.2 × 10^3 M^{-1}, ΔG^* = 12.8 kcal mol^{-1}, k_{off} = 2.5 × 10^3 s^{-1}), $ADPH^{2-}$ (K_a = 13 M^{-1}, ΔG^* = 12.1 kcal mol^{-1}, k_{off} = 7.7 × 10^3 s^{-1}), ATP^{4-} (K_a = 3.0 × 10^3 M^{-1}, ΔG^* = 12.4 kcal mol^{-1}, k_{off} = 5 × 10^3 s^{-1}), and $ATPH^{3-}$ (K_a = 6 M^{-1}, ΔG^* = 12.5 kcal mol^{-1}, k_{off} = 4.2 × 10^3 M^{-1}) have been determined by a total line shape analysis of ^{25}Mg NMR spectra. The results were compared with data previously determined for $tRNA^{Phe}$ (yeast) (Reid, S. S.; Cowan, J. A. *Biochemistry* **1990**, *29*, 6025-6032). Estimates of the on-rate for magnesium binding (k_{on} = K_a/k_{off}) were made; k_{on} (s^{-1}) = 4.3 × 10^4, 2.5 × 10^4, 1.4 × 10^4, 6.2 × 10^4, 5.5 × 10^6, 8.5 × 10^4, 1.5 × 10^7, 5.1 × 10^4, and 5.5 × 10^4, (tRNA), respectively. Outer-sphere association constants were also estimated; K_{os} (M^{-1}) = 0.43, 0.25, 0.14, 0.62, 55, 0.85, 150, 0.51, and 220 (tRNA), respectively. The exchange regime for Mg^{2+} binding shows no trend with K_a but appears to correlate with the number of inner- and outer-sphere binding contacts to $Mg(H_2O)_n^{2+}$. Magnesium binding to $ADPH^{2-}$ and $ATPH^{3-}$ occurs preferentially at the terminal phosphate dianion, and the α- or β-phosphate, respectively, is protonated. Possible relevance to the role of Mg^{2+} in enzymatic catalysis is discussed briefly. Magnesium binding to a terminal phosphate apparently leads to facile protonation of an inner phosphate that results in a reactive pyrophosphate-type center.

Introduction

Alkali-metal and alkaline-earth-metal ions (Na^+, K^+, Mg^{2+}, and Ca^{2+}) are the most abundant metal ions in biology; however, their biochemistry has received less attention than that of transition metals because the latter are more readily studied by common spectroscopic and electrochemical methods. Magnesium is a frequent cofactor for RNA and DNA processing enzymes, ribozymes, and an essential component of the ribosome.[1-8] It is important, therefore, to understand the manner in which magnesium binds to its "biological ligands" and activates them structurally and catalytically.[9] In aqueous solution, Mg^{2+} will typically form the hexahydrated $Mg(H_2O)_6^{2+}$ species; however, when it is bound to a protein or RNA, the inner and outer coordination environment is less well characterized. Magnesium readily forms complexes with biological substrates and may serve to either define a particular conformation or catalytically activate chemical functionality toward reaction.[10-16] The role of the metal

† Abbreviations: deoxyribonucleic acid (DNA); phenylalanine transfer ribonucleic acid ($tRNA^{Phe}$); adenosine monophosphate (AMP^{2-}); adenosine diphosphate (ADP^{3-}); adenosine triphosphate (ATP^{4-}); single strand (ss); double strand (ds); variable temperature (VT); room temperature (RT).

(1) Linn, S. M., Roberts, R. J., Eds. *Nucleases*; Cold Spring Harbor Laboratory: Cold Spring Harbor, NY, 1985.
(2) McClarin, J. A.; Frederick, C. A.; Wang, B.-C.; Greene, P.; Boyer, H. W.; Grable, J.; Rosenberg, J. M. *Science* **1986**, *234*, 1526-1541 (and references therein).
(3) Latham, J. A.; Cech, T. R. *Science* **1989**, *245*, 276.
(4) Been, M. D.; Cech, T. R. *Science* **1988**, *239*, 1412-1416.
(5) Guerrier-Takada, C.; Altman, S. *Science* **1984**, *223*, 285-286.
(6) Altman, S.; Guerrier-Takada, C.; Frankfort, H. M.; Robertson, H. D. In *Nucleases*; Linn, S. M., Roberts, R. J., Eds.; Cold Spring Harbor Laboratory: Cold Spring Harbor, NY, 1985; p 243.
(7) Moore, P. B. *Nature* **1988**, *331*, 223-227.
(8) Ryan, P. C.; Draper, D. E. *Biochemistry* **1989**, *28*, 9949-9956.
(9) Williams, R. J. P. *Q. Rev., Chem. Soc.* **1970**, 331.
(10) Oestreich, C. H.; Jones, M. M. *Biochemistry* **1967**, *6*, 1515-1519.
(11) Kluger, R.; Wasserstein, P. *Biochemistry* **1972**, *11*, 1544-1546.
(12) Kluger, R.; Wasserstein, P.; Nakaoka, K. *J. Am. Chem. Soc.* **1975**, *97*, 4298-4303.
(13) Cooperman, B. S. *Biochemistry* **1969**, *8*, 5005-5010.

0020-1669/91/1330-2740$02.50/0

ion may be critically dependent on the coordination environment that it adopts, and so it would be useful to have an understanding of the binding chemistry of Mg^{2+} in a biological context.

This work builds on a large, although often conflicting, body of kinetic, thermodynamic [e.g., reported binding constants (K_a's) for ATP^{4-} range from 3.0×10^3 to 5.5×10^4 M^{-1}],[12,17-26] and structural data determined in other laboratories. The kinetics of Mg^{2+} binding to adenosine phosphates was originally described in the seminal work of Eigen and co-workers,[27] while the location of metal-binding sites on a number of polyphosphate anions has been the subject of much controversy.[28-31] Metal-catalyzed hydrolysis of phosphate esters has been of interest for many years and will undoubtedly receive new impetus by the recent discovery of catalytic RNA.[3-6,10-16,32]

In this paper, we discuss the coordination properties of the magnesium complexes of glucose 1-phosphate, glucose 6-phosphate, acetyl phosphate, AMP^{2-}, ADP^{3-}, $ADPH^{2-}$, ATP^{4-}, $ATPH^{3-}$, and $tRNA^{Phe}$ (yeast). The wide divergence in reported values for many important coordination parameters may reflect, in some cases, a breakdown in the correlation between the physical parameter of interest and the indirect variable being monitored. There are few available methods for direct studies of the solution chemistry of divalent magnesium; however, we have found ^{25}Mg NMR spectroscopy to be a useful technique for investigating the chemistry of magnesium ion with biological substrates and macromolecules. Herein we report thermodynamic and kinetic constants for Mg^{2+} binding to phosphate ligands obtained by this method and also reevaluate previous work. In particular, we aim to (1) provide a rationale for the specificity of magnesium-binding sites; (2) discuss the nature of the resulting coordination geometry, whether inner sphere (direct magnesium–phosphate linkage) or

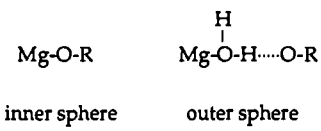

outer sphere (interaction through hydrogen bonding to a magnesium-bound water),[33,34] and (3) describe how the coordination chemistry may be controlled in a biochemically relevant fashion. Several discrepancies in the published literature are discussed. The relevance of this work for understanding the role of Mg^{2+} in enzymatic reactions is discussed in a final section.

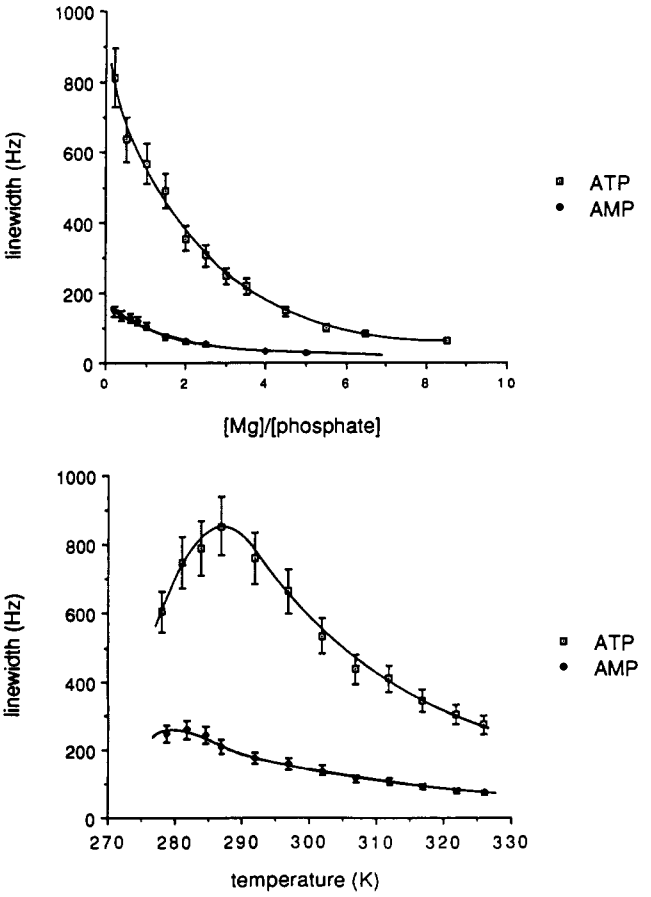

Figure 1. (A) Top: Magnesium titration curve obtained at 298 K (pH 7). General solution conditons: [ATP^{4-}] varied from 131 to 67 mM, [Mg^{2+}] varied from 31 to 426 mM; [AMP^{2-}] varied from 66 to 49 mM, [Mg^{2+}] varied from 16 to 258 mM. (B) Bottom: Variation of $\Delta\nu_{1/2}$-($^{25}Mg^{2+}$) with temperature. General solution conditions: [ligand] = 113 mM, [Mg^{2+}] = 177 mM (pH 7). Line-broadening factors of 50 and 10 Hz were used for ATP^{4-} and AMP^{2-}, respectively. The experimental points are shown relative to a theoretical curve obtained by joining calculated points from the fitting analysis.

Experimental Section

Materials. The sodium salts of $AMP(5')^{2-}$, ADP^{3-}, ATP^{4-}, glucose 1-phosphate, and glucose 6-phosphate and the mono(lithium/potassium) salt of acetyl phosphate were obtained from Sigma Chemical Co. and used without further purification. ^{25}MgO (98 atom % ^{25}Mg) was obtained from Oak Ridge National Laboratory. A stock solution of $^{25}Mg^{2+}$ (~0.1 M) was prepared from the oxide following titration with 1.0 M $HClO_4$ until the solution stabilized at pH 7. Solution pH's were measured by using an Accumet 910 meter (Fisher Scientific) equipped with a Ross combination pH electrode (Orion Research Inc.). Distilled water was deionized by passage through a Barnstead nanopure system.

^{25}Mg NMR Experiments. ^{25}Mg NMR spectra were recorded at 18.374 MHz on a Bruker MSL 300 spectrometer. Spectra were obtained without sample spinning by using the RIDE pulse sequence to reduce the effects of acoustic ringing.[35] Normally, two left shifts were applied to the data prior to Fourier transformation. A standard 0.3 M $MgCl_2$ solution gave a signal with a line width $\Delta\nu_{1/2}(^{25}Mg^{2+})_{free}$ = 2.8 Hz, in close agreement with literature precedent.[36] The 90° pulse width was 30 μs, while the acquisition times were 26 ms for broad lines and 171 ms

(14) Oestrich, C. H.; Jones, M. M. *Biochemistry* **1966**, *5*, 2926–2931.
(15) Briggs, P. J.; Satchell, D. P. N.; White, G. F. *J. Chem. Soc. B* **1970**, 1008–1012.
(16) Klinman, J. P.; Samuel, D. *Biochemistry* **1971**, *10*, 2126–2131.
(17) Smith, R. M.; Alberty, R. A. *J. Am. Chem. Soc.* **1956**, *78*, 2376–2380. Burton, K. *Biochem. J.* **1959**, *71*, 388–395.
(18) Pecoraro, V. L.; Hermes, J. D.; Cleland, W. W. *Biochemistry* **1984**, *23*, 5262–5271.
(19) Bock, R. M. In *The Enzymes*; Boyer, P. D., Lardy, H., Kyrback, K., Eds.; Academic: New York, 1960; pp 3–38. Phillips, R. *Chem. Rev.* **1966**, *66*, 501–527. Izatt, R. M.; Christensen, J. J.; Rytting, J. H. *Chem. Rev.* **1971**, *71*, 439–481.
(20) Khan, M. M. T.; Martell, A. E. *J. Phys. Chem.* **1962**, *66*, 10–15.
(21) Khan, M. M. T.; Martell, A. E. *J. Am. Chem. Soc.* **1962**, *84*, 3037–3041. Kahn, M. M. T.; Martell, A. E. *J. Am. Chem. Soc.* **1966**, *88*, 668–671. Kahn, M. M. T.; Martell, A. E. *J. Am. Chem. Soc.* **1967**, *89*, 5585–5590.
(22) Rose, D. M.; Bleam, M. L.; Record, M. T.; Bryant, R. G. *Proc. Natl. Acad. Sci. U.S.A.* **1980**, *77*, 6289–6292. Bleam, M. L.; Anderson, C. F.; Record, M. T. *Proc. Natl. Acad. Sci. U.S.A.* **1980**, *77*, 3085–3089.
(23) Scheller, K. H.; Hofstetter, F.; Mitchell, P. R.; Prijs, B.; Sigel, H. *J. Am. Chem. Soc.* **1981**, *103*, 247–260.
(24) Diebler, H.; Eigen, M.; Ilgenfritz, G.; Maab, G.; Winkler, R. *Pure Appl. Chem.* **1969**, *20*, 93–115.
(25) Frey, C. M.; Stuehr, J. E. *J. Am. Chem. Soc.* **1972**, *94*, 8898–8904.
(26) Frey, C. M.; Banyasz, J. L.; Stuehr, J. E. *J. Am. Chem. Soc.* **1972**, *94*, 9198–9204.
(27) Eigen, M.; Hammes, G. G. *J. Am. Chem. Soc.* **1961**, *83*, 2786.
(28) Melchior, N. C. *J. Biol. Chem.* **1954**, *208*, 615–627. Epp, A.; Ramasarma, T.; Wetter, L. R. *J. Am. Chem. Soc.* **1958**, *80*, 724–727.
(29) Huang, S. L.; Tsai, M.-D. *Biochemistry* **1982**, *21*, 951–959.
(30) Cohn, M.; Hughes, T. R. *J. Biol. Chem.* **1960**, *235*, 3250–3253. Cohn, M.; Hughes, T. R. *J. Biol. Chem.* **1962**, *237*, 176–181.
(31) Jaffe, E. K.; Cohn, M. *Biochemistry* **1978**, *17*, 652–657.
(32) Guerrier-Takada, C.; Gardiner, K.; Marsh, T.; Pace, N.; Altman, S. *Cell* **1983**, *35*, 849.
(33) Burgess, J. *Ions in Solution: Basic Principles of Chemical Interaction*; Ellis Horwood Ltd.; New York, 1988; Chapter 10.
(34) Frey, C. M.; Stuehr, J. *Met. Ions Biol. Syst.* **1974**, *1*, 51–115.
(35) Ellis, P. D. In *The Multinuclear Approach to NMR Spectroscopy*; Lambert, J. B., Riddell, F. G., Eds.; Reidel: Boston, MA, 1983; pp 425–523.
(36) Lindman, B.; Forsen, S.; Lilja, H. *Chem. Scr.* **1977**, *11*, 91.

for narrow lines (spectral widths of 20 000 Hz and 3000 Hz, respectively) with a preacquisition delay of 100 μs. A Lorentzian line broadening of 10–50 Hz was typically applied to data, depending on the experiment.

Magnesium or pH titration and variable-temperature (VT) experiments generally used less than 0.5 mmol of ligand. Specific experimental procedures for studies of tRNA have been described previously.[37,38] Titration experiments were carried out at 298 K, with successive additions from the stock solution of $^{25}Mg^{2+}$. In the later portion of the titration, when a good signal/noise ratio was attainable within a reasonable time period, additions of Mg^{2+} were made from a 1 M $MgCl_2$ solution containing natural-abundance $^{25}Mg^{2+}$. In all cases, the concentrations of stock solutions were accurately determined by atomic absorption. Variable-temperature experiments (from 5 to 55 °C) were performed with a fixed $[Mg^{2+}]/[ligand]$ ratio, and values for $\Delta\nu_{1/2}(^{25}Mg^{2+})$ obtained both before and after heating were similar.

Data Analysis. The NMR line shape analysis programs employed in this study were written by Dr. Torbjorn Drakenberg (Lund, Sweden) and have been described in greater detail elsewhere.[37-41] Association constants (K_a) and activation energies (ΔG^*) were determined by following procedures described previously.[37,39] Several parameters are required to fully define the line shape of a resonance. These include the chemical shifts of free and bound ions [normally $\delta(^{25}Mg^{2+})_{free} \sim \delta(^{25}Mg^{2+})_{bound}$]. The relative populations of $(Mg^{2+})_{free}$ and $(Mg^{2+})_{bound}$ are dependent on $[Mg^{2+}]$, [ligand], and the binding constant K_a, and so these parameters are introduced into the analysis routine. The temperature dependence of k_{off} is assumed to follow standard transition-state theory [$k_{off} = (kT/h)\, e^{-\Delta G^*/RT}$]. This manifests itself through the dependence of $\Delta\nu_{1/2}(^{25}Mg^{2+})$ on the relative rate of exchange between free and bound $^{25}Mg^{2+}$. Low molecular weight complexes have a correlation time τ_c in solution of $\sim 10^{-9}$–10^{-10} s (a value of 0.4 ns was typically used), while that for tRNA is larger ($\tau_c \sim 24.5$ ns) and has been considered in detail elsewhere.[37] In each case, these values fall within an acceptable range for the analysis routine.[39,40] Several problems arising in ^{25}Mg NMR studies on larger biological macromolecules have been outlined in detail elsewhere.[22,37-41] Under conditions where $\tau_c\omega_0 \leq 1.5$, such as found for most small biological macromolecules and all smaller substrate ligands, the ^{25}Mg NMR line shapes has Lorentzian form (the relaxation properties of all possible transitions are effectively equivalent).[40] The analysis program employed does not, however, assume a Lorentzian line form. For large molecules that bind Mg^{2+} strongly ($K_a > 10^4$ M^{-1}), the resonance from the Mg^{2+} complex may be too broad to detect. This is not the case in this study. Integration of resonances demonstrated that all of the signal was observable for all metal/ligand ratios; even when less than 1 equiv of $^{25}Mg^{2+}$ was added (Figure 1).

Data were analyzed by an iterative least-squares fit of digitized NMR spectra. Zero filling was employed where necessary to better define the peak. Typically, each spectrum was defined by 30 points and the best combination of ΔG^*, χ_B, and K_a was found by an iterative procedure. Consideration of the variation of $\Delta\nu_{1/2}(^{25}Mg^{2+})$ with $[Mg^{2+}]/[ligand]$ and temperature gives values for the association constant (K_a), quadrupole coupling constant (χ_B), activation free energy (ΔG^*), and the off-rate (k_{off}).[39] Titration and VT data must be analyzed cyclically to give the best fit because of the interdependence of equations containing K_a, χ_B, and ΔG^* as variables.[38] The analysis routine, considering all data sets, gives rise to unique values for each of the aforementioned parameters; however, the individual enthalpic and entropic components of the activation energies for the monophosphate complexes are most likely unreliable, since ΔH^* is defined by the slope and inflection in the slow–intermediate exchange region of the VT plot. For this reason, the relative values of ΔH^* and ΔS^* are not considered. A Lorentzian line-broadening function of 10–50 Hz was applied to data prior to Fourier transformation. Since this is only a fraction of the total range of natural line widths, which typically vary from 30 to 800 Hz (see Figure 1), a minimal error is introduced.

pH Titrations. The pK values for the titration steps in $\Delta\nu_{1/2}(^{25}Mg^{2+})$ vs pH plots were obtained by fitting appropriate data sets to an equation defining a single ionization equilibrium $[\Delta\nu_{1/2}(pH) = \Delta\nu_{1/2}(HA)[H^+]/(K + [H^+]) + \Delta\nu_{1/2}(A^-)K/(K + [H^+])]$ with the use of a nonlinear least-squares program. We reserve use of the symbol K_a to denote the constant for Mg^{2+} binding to a specified ligand. Acidity constants are generally listed in logarithmic notation as pK values and refer to the reported solution conditions. The use of subscripts (e.g. pK_1, pK_2, etc.) will refer to either first or second ionizations, etc., to be explicitly defined in the text. The pK_1 and pK_2 notation is used in references to ionization of a terminal phosphate group and do not denote ionization of ring protons or the inner phosphates of a multiphosphate anion.

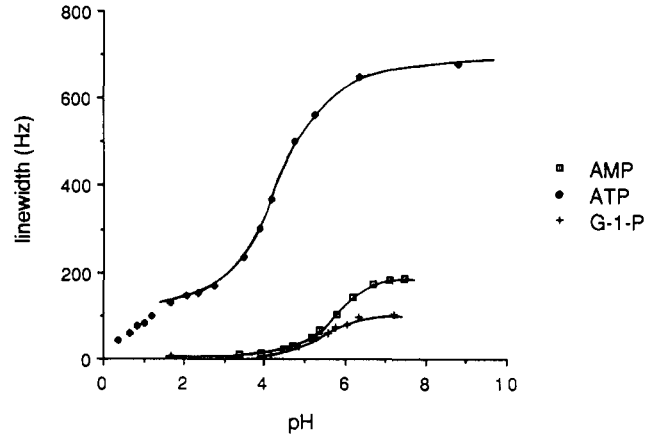

Figure 2. Variation of $\Delta\nu_{1/2}(^{25}Mg^{2+})$ vs pH for glucose 1-phosphate, AMP^{2-}, and ATP^{4-}. The concentrations of ligand and magnesium were ca. 130 and 100 mM, respectively, at 298 K.

Table I. Determination of Kinetic and Thermodynamic Parameters for Magnesium Binding to Phosphate-Containing Ligands by ^{25}Mg NMR Spectroscopy[a]

ligand	K_a, M^{-1}	ΔG^*, kcal mol^{-1}	$10^{-3}k_{off}$,[b] s^{-1}	k_{on}, s^{-1}	K_{os}, M^{-1}
$tRNA^{Phe}$ (native)[c]	220	12.8	2.5	5.5×10^5	220
$tRNA^{Phe}$ (nonnative)[c]	250	13.1	1.6	4.0×10^5	250
$[glucose\text{-}1\text{-}P]^{2-}$	15	12.7	2.9	4.3×10^4	0.43
$[glucose\text{-}6\text{-}P]^{2-}$	8	12.7	3.1	2.5×10^4	0.25
$CH_3CO_2PO_3^{2-}$	9	13.1	1.5	1.4×10^4	0.14
AMP^{2-}	18	12.7	3.4	6.2×10^4	0.62
ADP^{3-}	2.2×10^3	12.8	2.5	5.5×10^6	55
$ADPH^{2-}$	13	12.1	7.7	8.5×10^4	0.85
ATP^{4-}	3.0×10^3	12.4	5.0	1.5×10^7	150
$ATPH^{3-}$	6	12.5	4.2	5.1×104	0.51

[a] Estimated errors in K_a and ΔG^* are ±10–20% and ±0.2 kcal mol^{-1}, respectively. Values for k_{off}, k_{on}, and K_{os} were determined from these parameters (taking $T = 298$ K) as follows: $k_{off} = kT/h \exp(-\Delta G^*/RT)$; $k_{on} = K_a k_{off}$; $K_{os} = k_{on}/k_i$, where k_i is taken as 10^5 s^{-1}.[33] [b] Some differences will be noted in values for k_{off} that correspond to apparently identical ΔG^* data (Column 3). This arises from "rounding-off" errors. [c] Data were obtained at 303 K.[37]

Atomic Absorption. Measurements of magnesium ion concentration (±2.5%) were made on a Perkin-Elmer atomic absorption spectrometer (AA) using an air/acetylene fuel mixture. The Mg lamp was operated at 285.2 nm, slit width 0.7 nm, and the instrument was calibrated against a series of solutions containing 0.1, 0.3, and 0.5 ppm of Mg^{2+}, prepared by successive dilutions of a standard solution 1000 ppm in Mg^{2+} (GFS Chemicals). Volumetric glassware was pretreated with an acid wash. Known volumes of the magnesium stock solutions were diluted to give an approximate concentration between 0.15 and 0.5 ppm in Mg^{2+}.

Results and Discussion

Magnesium titration and VT experiments on low molecular weight complexes were carried out at both pH 7.5 and 3.0, where the phosphate unit is fully ionized and monoprotonated, respectively (Figure 2). Kinetic and thermodynamic parameters derived from line shape analyses are noted in Table I. The thermodynamics of metal binding has been reviewed extensively;[19] therefore, in this paper we shall emphasize distinct aspects of the chemistry (viz., specificity of the coordination site, the influence of Mg^{2+} on protonation sites, and the activation of pyrophosphate-type anions toward nucleophilic attack). Binding data from low molecular weight complexes are also compared with results obtained for $tRNA^{Phe}$ (yeast).[37]

Binding Thermodynamics. By fits of both the Mg^{2+} titration and VT plots (Figure 1), values for K_a and ΔG^* were determined by iteratively optimizing each in a cyclic manner. At room tem-

(37) Reid, S. S.; Cowan, J. A. *Biochemistry* **1990**, *29*, 6025–6032.
(38) Drakenberg, T.; Forsen, S.; Lilja, H. *J. Magn. Reson.* **1983**, *53*, 412–422.
(39) Tsai, M.-D.; Drakenberg, T.; Thulin, E.; Forsen, S. *Biochemistry* **1987**, *26*, 3635–3643.
(40) Halle, B.; Wennerstrom, H. *J. Magn. Reson.* **1981**, *44*, 89–100.
(41) Blank, G. *Acta Crystallogr.* **1973**, *B29*, 1677–1683.

perature (RT), free and complexed Mg^{2+} are in fast exchange for each of the low molecular weight ligands. Values of $\Delta\nu_{1/2}(^{25}Mg^{2+})$ for ADP^{3-} and ATP^{4-} were typically much broader than those for monophosphate derivatives, reflecting stronger binding to these chelating ligands. K_a's for the monophosphate derivatives were similar (8–18 M^{-1}; Table I), and comparison of the results for glucose phosphates, AMP^{2-}, and acetyl phosphate suggests that the hydroxyls on the sugar units do not play an important role in complexing Mg^{2+}, relative to the phosphate head group. Coordination of both Mg^{2+} and Ca^{2+} by the sugar hydroxyls of a number of carbohydrate molecules has been demonstrated by crystallography[41-43] and has been implicated in the transmission of nerve signals, changes in membrane structure, and bone formation.[41-43] Evaluation of K_a's (Table I) for ADP^{3-} and ATP^{4-} by the direct NMR method gives results that are up to 3–10 times smaller than those determined by spectrophotometric, electrochemical, and pH titrimetric methods. Whatever the value determined in solution, it is important to realize that the effective K_a for metal–ligand coordination is likely to be much greater in an environment of low dielectric constant, such as a protein or membrane binding site. A potential source of error in our measurements that is not readily accounted for by ^{25}Mg NMR spectroscopy is the effect of aggregation between nucleotides. Using the association constants of Sigel and co-workers, we estimate dimer formation to be ca. 2–8% for the ligand concentrations employed in this work (typically 10–100 mM).[23] Given the errors involved, small influences on metal binding constants could easily go undetected. Such interactions are readily detected by ^{31}P NMR and ^{1}H NMR spectroscopy.[18,23] However, the ^{25}Mg data could be readily fit by assuming one type of binding domain and were not significantly improved by assuming a second minor site. In the case of macromolecules in particular, deviations of line shapes from Lorentzian form can complicate the analysis as a result of partial invisibility of resonances and/or complex relaxation behavior. Such effects do not arise here. Furthermore, smaller ligands demonstrating tight magnesium binding may result in the loss of signal as a result of resonances broadened beyond detection. Again, for the reasons discussed earlier, this did not appear to be an issue for our work. An additional source of error arises from the dependence of K_a on temperature; however, it has been previously shown that this varies by less than a factor of 2 in the temperature range employed in these experiments.[21] Any correction to the activation energies as a result of this difference is minor and is within the quoted error limits (Table I). Although this deviation is not insignificant, and larger than reported errors arising from indirect methods,[18] there is a concern that the variable being measured in the latter type of experiment does not truly represent the binding chemistry of interest. Brown and co-workers have established that neither IR spectroscopy nor methods dependent on pH measurement can provide reliable values for binding constants, since there may not be a direct correspondence between proton displacement and metal binding.[44] Early attempts to determine values for K_a have been the subject of an extremely critical but perceptive review by Bock.[19]

The values of K_a determined by ^{25}Mg NMR spectroscopy for Mg^{2+} complexes with monophosphates are similar (Table I). Our value for acetyl phosphate ($K_a \sim 9$ M^{-1}) is in reasonable agreement with the results of Kluger and co-workers ($K_a \sim 6$ M^{-1}) and Oestreich and Jones ($K_a \sim 8.2$ M^{-1}).[12,14] Two binding constants have been reported for glucose 1-phosphate ($K_a \sim 20$ M^{-1} and $K_a \sim 305$ M^{-1}).[45-47] The relatively weak coordination by these ligands serves to emphasize the remarkable binding of Mg^{2+} by tRNA that achieves a $K_a = 250$ M^{-1} for each of the "weak" Mg^{2+} coordination sites but possesses a series of backbone phosphodiesters as the only phosphate-bearing ligand.[37] Normally, phosphodiesters show $K_a < 6$ M^{-1}. For each low molecular weight

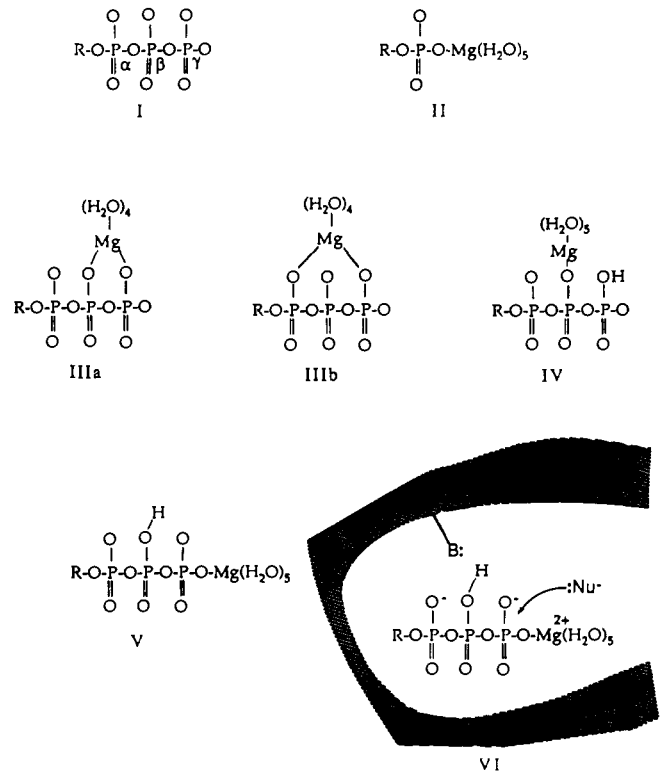

Figure 3. Possible coordination structures for Mg^{2+}–polyphosphate complexes referred to in the text (R denotes a general group but frequently refers to adenosyl). Except for VI, formal charges on the magnesium ion and phosphate oxygen have been omitted for clarity.

complex, $\Delta\nu_{1/2}(^{25}Mg^{2+})$ demonstrated no dependence on background salt concentration ($Na^+(aq)$ and $K^+(aq)$) between 5 and 400 mM, indicating a large specificity for the interaction of phosphate with Mg^{2+} relative to monovalent alkali-metal ions. This is in contrast to data obtained by methods relying on pH measurement where Na^+ and K^+ can compete with H^+, and results should be extrapolated to infinite dilution. We have proposed elsewhere that Mg^{2+} will most commonly bind to ds RNA as an outer-sphere complex, retaining its full solvation shell and forming an extensive H-bonding network to backbone phosphates, nucleotide bases, and sugar hydroxyls.[37,48] Low molecular weight complexes on the other hand typically form inner-sphere complexes with Mg^{2+}. An appropriate comparison of magnesium-binding data for RNA and smaller ligands is through the value of K_a for tRNA and the outer-sphere association constant K_{os} for low molecular weight phosphates.[49,50] In comparison to those of typical phosphodiester ligands, the increased association constant for tRNA reflects, in part, this distinct binding mode for the metal ion and also the greater electrostatic interaction with the polynucleotide backbone. The relative values of K_{os} listed in Table I correlate with the ability of each ligand to form an H-bonding network to divalent hexaaquomagnesium(II) $[Mg(H_2O)_6]^{2+}$ (discussed below). In particular, if the possibility of multiple hydrogen-bond contacts from $[Mg(H_2O)_6]^{2+}$ to O and N atoms on the ribose sugars and oligonucleotide base units is considered, the difference in coordination can be understood simply on the basis of total bond energies.[48] In this regard, it is important to note that the results derived from this type of analysis represent the effective values of thermodynamic parameters at a local site. It is not, however, assumed that the binding energy derives totally from a local set of binding constraints (e.g., electrostatic interactions with a particular backbone phosphate). Our approach does not neglect the central tenets of polyelectrolyte theory but assumes that other binding mechanisms (particularly the H-bond

(42) Cook, W. J.; Bugg, C. E. *J. Am. Chem. Soc.* **1973**, *95*, 6442–6446.
(43) Cook, W. J.; Bugg, C. E. *Biochim. Biophys. Acta* **1975**, *389*, 428–435.
(44) Khalil, F. L.; Brown, T. L. *J. Am. Chem. Soc.* **1964**, *86*, 5113–5117.
(45) Tabor, H.; Hastings, A. B. *J. Biol. Chem.* **1943**, *148*, 627.
(46) Datta, S. P.; Grzybowski, A. K. *Biochem. J.* **1958**, *69*, 218.
(47) Clarke, H. B.; Cusworth, D. C.; Datta, S. P. *Biochem. J.* **1954**, *58*, 146.
(48) Cowan, J. A. *J. Am. Chem. Soc.* **1991**, *113*, 675–676.
(49) Eigen, M.; Tamm, K. *Z. Elektrochem.* **1962**, *66*, 93–121.
(50) Eigen, M.; Tamm, K. *Z. Elektrochem.* **1962**, *66*, 107.

network) are also operative. Polyelectrolyte theory does not account for such interactions. The values we determine may therefore be regarded as good experimental approximations to allow the field to progress, while identifying weaknesses in assumptions inherent to current theoretical approaches.

Structure of the Mg(ATP^{4-}) Chelate. As a result of the importance of the Mg(ATP^{4-}) complex in enzyme-catalyzed phosphoryl-transfer reactions, the structure of this species has been widely discussed in the literature. Every possible coordination mode from monodentate through tridentate has been proposed. In this brief section we critically review the available evidence and reason that only structures IIIa,b in Figure 3 are acceptable candidates for this complex. It is not necessary to differentiate between these two possibilities to understand the results discussed below; however, some comments are clearly in order.

Monodentate complexes may be eliminated on the basis of the large binding constant noted for Mg(ATP^{4-}). Tridentate coordination may also be eliminated for the following two reasons: (1) most data sets show a similarity between K_a for ATP^{4-} and ADP^{3-} that is not supportive of tridentate vs bidentate coordination; (2) a single protonation step results in a reduction in K_a to a value similar to that for a monophosphate ligand, which would not be expected for a tridentate ligand. Consequently, only the three bidentate chelate structures need be considered. Coordination to the terminal γ-phosphate has been unequivocally established,[31] and so only IIIa,b in Figure 3 remain as viable candidates. Cohn and co-workers previously obtained evidence for coordination to the β,γ-phosphate unit by ^{31}P NMR spectroscopy but later expressed concern with the reliability of the method because shifts were also noted in ^{31}P resonances for phosphate units adjacent to putative Mg^{2+} coordination sites,[28-31] presumably due to an electronic influence on adjacent ^{31}P nuclei. However, such changes can also be readily accounted for by H-bonding interactions between Mg^{2+}-bound H_2O and the adjacent phosphate oxygen. Furthermore, the pH titration data for the Mg(ATP^{4-}) complex presented in the earlier work of Cohn and Hughes provide strong support for a β,γ-coordination mode.[30] While it is difficult to completely rule out the possibility of structure IIIb, the ^{31}P and ^{17}O NMR data supporting such a geometry can also be easily rationalized by IIIa and an H-bonding interaction from Mg^{2+}-bound H_2O to the α-phosphate.[29] For the purposes of this paper, we assume structure IIIa; however, many of the arguments do not depend on this and are equally valid for IIIb. Some of our data (below) do, however, provide further support for the former.

Influence of pH on Binding. The variation of $\Delta\nu_{1/2}(^{25}Mg^{2+})$ with pH can be used to monitor the influence of Mg^{2+} on the acidity constants (pK's) for ligand functionality in the vicinity of metal-binding sites (Figure 2). In the presence of 100 mM Mg^{2+}, the monophosphate ligands show pK's of ca. 5.5–5.8 (Table II). Both ADP^{3-} and ATP^{4-} show a shift in the measured pK values (4.61 and 4.33, respectively) following binding of Mg^{2+} (Table II). Normally, pK values for the second ionization of the terminal phosphate range from 6.2 to 6.9 for the free ligands, while acidity constants for the central phosphate are typically <2. Protonation of ionizable groups on the adenine ring do not appear to influence Mg^{2+} binding. The variation of $\Delta\nu_{1/2}(^{25}Mg^{2+})$ vs pH for ATP^{4-} is different from that previously reported in a ^{25}Mg NMR study,[51] although this may reflect the larger concentrations of Mg^{2+} employed due to limitations on available instrumentation at that time. An additional inflection at pH <2 was observed for Mg(ATPH^{3-}) that may be attributed to further protonation (pK_1) of the terminal phosphate (with displacement of Mg^{2+}). However, Mg(ADPH^{2-}) shows no obvious inflection, and so the effect is either less prominent, or the pK_1 for this complex is at lower pH, or protonation of Mg(ADPH^{2-}) actually occurs at the α-phosphate adjacent to the ring. The latter is unlikely since it would implicate contact between the metal ion and the α-phosphate (see discussion above and refs 29–31). Although it is possible to form an H-bond to the α-phosphate following rotation of the middle phosphate groups, the metal should still bind to the γ-phosphate. This is in contrast to what is actually observed, since $\Delta\nu_{1/2}(^{25}Mg^{2+}) \rightarrow \Delta\nu_{1/2}(^{25}Mg^{2+})_{free}$ upon lowering the pH and is accompanied by release of Mg^{2+}.

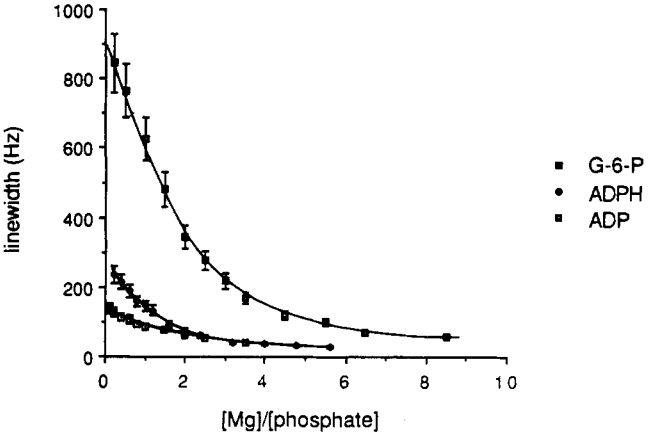

Figure 4. Comparison of magnesium titration curves for glucose 6-phosphate (pH 7), ADP^{3-} (pH 7), and ADPH^{2-} (pH 3). Other experimental conditions were similar to those in the caption to Figure 1.

The variation of $\Delta\nu_{1/2}(^{25}Mg^{2+})$ as a function of $[Mg^{2+}]$ is shown at pH 7.5 and pH 3.0 in Figure 4 for ADP^{3-} (ATP^{4-} is similar). At pH 3, ADPH^{2-} and ATPH^{3-} apparently lose their chelating ability and the K_a's ($\sim$13 and 6 M^{-1}, respectively) are comparable to those for monophosphates, even though each retains functionality able to chelate the metal ion (e.g. Figure 3, IV). In keeping with this observation, the monophosphate ligands bind Mg^{2+} ineffectively ($K_a \leq 1$ M^{-1}) at low pH [$\Delta\nu_{1/2}(^{25}Mg^{2+}) \rightarrow \Delta\nu_{1/2}(^{25}Mg^{2+})_{free}$]. These results show the same trend as previous literature reports;[21,26] however, the discrepancy concerning the apparent large decrease in binding constant while the bis(phosphate) chelating functionality is retained (Figure 3, I) has not been addressed. It is unlikely that the terminal phosphate itself binds in a tight chelating fashion.[52-54] Rather, direct binding to one of the terminal phosphate oxygens (Figure 3, II) or additional chelation to the $\beta(\alpha)$-phosphate in AT(D)P$^{4(3)-}$, respectively (Figure 3, III), appears more reasonable. The large decrease in K_a for Mg^{2+} binding to mono-, di-, and triphosphates following protonation in a biologically relevant pH range raises important implications for magnesium phosphate interactions in vivo. This point is therefore considered in some detail. It has previously been noted that the pK's for these ligands decrease in the presence of Mg^{2+}.[44] This is further demonstrated by the ^{25}Mg NMR data in Figure 2 and by the ^{31}P NMR measurements of Cohn and Hughes,[30] which show a shift in the pK for the γ-phosphate of ATP. After careful inspection of the published data, however, it is clear that the middle β-phosphate is also titrating in the same pH range. This is unusual. On the basis of pH titration studies, one would normally expect the pK for the β-phosphate to be <2. Crutchfield and co-workers have argued that simple indirect titration studies can be misleading, since they do not show the site of protonation, and have demonstrated by use of ^{31}P NMR spectroscopy that the middle phosphates in polyphosphate anions[56] are also significantly protonated in the pH range 5–7.[55,56] This may result either from the acidic proton exchanging between the terminal and inner phosphates or by formation of a bridge between terminal and inner phosphates. The latter is particularly attractive, both from the viewpoint of explaining the observed changes in Mg^{2+} binding constants and also as an inherently reasonable structural arrangement. A bridging acidic proton in ADPH^{2-} and ATPH^{3-} would force Mg^{2+} to bind to the terminal phosphate unit, which therefore behaves as a monophosphate ligand (V, Figure

(51) Bryant, R. G. *J. Magn. Reson.* **1972**, *6*, 159–166.

(52) Brintzinger, H. *Helv. Chim. Acta* **1961**, *45*, 935–939.
(53) Brintzinger, H. *Biochim. Biophys. Acta* **1963**, *77*, 343–345.
(54) Martell, A. E.; Schwarzenbach, G. *Helv. Chim. Acta* **1956**, *39*, 653–661.
(55) Crutchfield, M. M.; Callis, C. F.; Irani, R. R.; Roth, G. C. *Inorg. Chem.* **1962**, *1*, 813–817.
(56) The discussion of $P_3O_{10}^{5-}$ is particularly relevant.

3). This type of bridging or H-bonding interaction would also readily explain the unusual shifts observed in ^{31}P NMR signals of phosphate following protonation of adjacent phosphate units.[31] Protonation of the terminal β- or γ-phosphate, respectively, with displacement of Mg^{2+} to the adjacent inner phosphate (IV, Figure 3), would appear to be a reasonable alternative, since the inner phosphate oxygens are inherently weak Lewis bases and should bind Mg^{2+} less strongly, as observed. However, Mg^{2+} is a harder Lewis acid than H^+ and would be expected to bind to the most basic site (highest pK), i.e. the terminal phosphate. The metal-binding site for this ligand anion should therefore be predictable from consideration of hard-acid/hard-base interactions. This conclusion contradicts that of Pecoraro et al., who favored IV (Figure 3) on the basis of the greater shift in the ^{31}P resonance of the terminal phosphate following protonation of the ligand.[18] There is, however, no reason to expect that a breakdown in the chelate structure (IIIa converting to V, Figure 3) would not have the same effect and just as easily support the quoted data.[31] The argument in favor of protonation of the β- versus the γ-phosphate of $Mg(ATP^{4-})$ can be extended as follows. If the γ-phosphate is indeed protonated, then the magnesium ion must either (1) bind to the β-phosphate, (2) form a chelate with the α- and β-phosphates, (3) bind to the remaining γ-phosphate oxygen, or (4) form a chelate with the β- and γ-phosphates. Each of these can be refuted by rational argument: (1) Binding constants are comparable to those determined for a terminal phosphate rather than a phosphodiester linkage. Furthermore, direct coordination of a divalent metal to a doubly charged phosphate should be a more stable configuration on electrostatic grounds. (2) ADP^{3-} also binds Mg^{2+} after protonation and cannot form such a chelate complex. (3) Protonation of monophosphates results in loss of Mg^{2+}; therefore, H^+ and Mg^{2+} cannot both bind to the terminal phosphate. (4) On the basis of the response to point 3, it is likely that Mg^{2+} would interact weakly with the γ-phosphate and bind principally to the β-phosphate, which has already been discussed under point 1. In the context of binding to ATP^{4-}, a reasonable compromise between IV and V in Figure 3 is that H^+ lies mostly on the β-O, perhaps forming a weak H-bond to the γ-phosphate, while Mg^{2+} interacts specifically with the terminal γ-phosphate unit.

Protonation of simple monophosphate ligands results in a weak basic ligand (pK < 2) with low affinity for Lewis acids; thus, such ligands show a corresponding decrease in Mg^{2+}-binding affinity ($K_a \sim 1\ M^{-1}$). This lends further support to the metal-induced protonation of the phosphate adjacent to the terminal unit in di- and triphosphates, rather than the remaining terminal phosphate oxygen, since K_a for $ADPH^{2-}$ and $ATPH^{3-}$ is comparable to binding constants for monophosphate dianions. The metal center has a profound influence on the reactivity of the ligand: protonation results in a substantial change in the affinity and location of the Mg^{2+}-binding site. *It is also clear that Mg^{2+} will influence the location of the protonation site.*

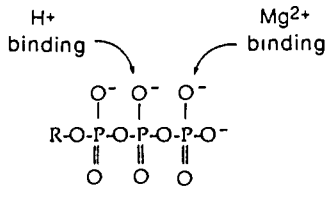

Such changes may constitute useful mechanisms to direct and trigger the uptake or release of divalent magnesium from substrate complexes and are most likely involved in the chemical activation of polyphosphate ions toward nucleophilic attack. The relevance of these observations to biochemical reactions of phosphates will be discussed further in the section on "Binding Chemistry".

Kinetics of Binding. The temperature plots fall into three distinct categories. Low molecular weight phosphates are always in rapid exchange at ambient temperatures and only show intermediate behavior at ca. 0–5 °C. Chelating ligands such as ADP^{3-} and ATP^{4-} show slow to intermediate exchange of Mg^{2+} that moves to fast exchange with increasing temperature (Figure 1B). Our measured dissociation rate ($k_{off} \sim 2.5 \times 10^3\ s^{-1}$, Table I) for ADP^{3-} is in good agreement with previous determinations by temperature-jump experiments.[25-27] The value for ATP^{4-} ($k_{off} \sim 5.0 \times 10^3\ s^{-1}$, Table I) compares to the value ($k_{off} \sim 1.2 \times 10^3\ s^{-1}$) determined by Eigen and Hammes[27] but is intermediate between the results of Frey et al. and Bryant,[25,26,51] who determined values of 7.2×10^2 and $2 \times 10^4\ s^{-1}$ by temperature jump and ^{25}Mg NMR spectroscopy, respectively. The possible formation of bis(magnesium) complexes (Mg_2ATP) and exchange with an ATP dimer have been put forward as explanations for the larger value determined by Bryant, whose measurements were carried out at high $[Mg^{2+}]$ ($\sim$1.5 M).[18,26] At low pH, $ADPH^{2-}$ and $ATPH^{3-}$ show temperature profiles similar to those for monophosphates (not shown), supporting the loss of a chelating unit.

Magnesium-binding sites on tRNA show slow exchange at RT,[37] moving through intermediate to fast exchange with increasing temperature. It is assumed that the large majority of weak-binding sites have similar ligand environments, and so we have previously argued that this should be reflected in the binding parameters.[37] The apparently complex folded structure of the molecule should not be confused with the relatively simple ds RNA and ss loop RNA from which it is constructed.[57] Furthermore, Mg^{2+} binds firmly to RNA with little internal motion [i.e., $\tau_c(Mg^{2+})_{bound} \sim \tau_c(RNA)$],[48] and so this does not compromise the data. It follows that a large range of K_a, ΔG^*, and ΔH^* would not be expected for the bound ions and that these parameters are approximately constant for each site. The very small number of unusual binding sites that do exist would not significantly influence the overall results derived from the analysis.[57]

We now address an interesting question. What factors determine the profile of a VT plot; i.e., what factors govern the transition temperature where a metal complex will move from slow, through intermediate, to fast exchange? Magnesium is normally in slow exchange with RNA or proteins at RT, whereas exchange is rapid with low molecular weight complexes. The trend does not depend on whether an inner- or outer-sphere coordination mode is adopted, since proteins will generally bind Mg^{2+} by direct inner-sphere contacts from the protein residues to the metal ion.[58,59] Furthermore, the exchange regime cannot be correlated with K_a, since both ADP^{3-} and ATP^{4-} bind Mg^{2+} with $K_a > 10^3\ M^{-1}$, in contrast to the weaker complex with RNA. A possible explanation is that the exchange regime for metal binding is determined by the total number of binding contacts to the aquated Mg^{2+} center, either inner or outer sphere. Both RNA and protein complexes typically form $\geq$4 binding contacts with $Mg(H_2O)_n^{2+}$, which is not the case for the low molecular weight phosphate ligands used in this study.[37,48,56-60]

Since the landmark measurements of Eigen and co-workers,[24,27] the kinetics of complexation have been investigated by few workers (Frey and Stuehr have provided a good review[34]) relative to the determination of thermodynamic parameters and the study of catalytic chemistry. Relevant data have been listed in Table I. Values for k_{off} are similar for each class of ligand, while deviations in k_{on} arise through the dependence on binding constants ($k_{on} = K_a k_{off}$). It is necessary to distinguish between the binding of metal ions to the low molecular weight phosphate ligands and binding to tRNA. In the former, an inner-sphere complex is formed, whereas outer-sphere coordination to RNA is suggested by crystallography and solution NMR studies.[37,48,57] The inner-sphere substitution chemistry of Mg^{2+} follows the modified Eigen–Tamm interchange mechanism:[34,49,50]

$$[Mg(H_2O)_6]^{2+} + L^- \overset{K_a}{\rightleftharpoons} [Mg(H_2O)_6,L^-]^+ \xrightarrow{k_i} [Mg(H_2O)_5,L^-]^+ + H_2O$$

(57) Jack, A.; Ladner, J. E.; Brown, R. S.; Klug, A. *J. Mol. Biol.* **1977**, *111*, 315–328.
(58) Szebenyi, D. M. E.; Moffat, K. In *Calcium-Binding Proteins*; de Bernard, B., et al., Eds.; Elsevier: Amsterdam, 1983; pp 199–205.
(59) Herzberg, O.; James, M. N. G. *Nature* **1985**, *313*, 653–659.
(60) These proteins normally bind Ca^{2+}. It is assumed that the coordination environment is similar for Mg^{2+}.

Table II. Influence of Mg^{2+} on the pK's for Protonation of Adenosine and Glucose Phosphates

ligand	pK^a	$pK(+Mg^{2+})^b$	pK_r^c
$[glucose\text{-}1\text{-}P]^{2-}$	6.5[d]	5.8	
$[glucose\text{-}6\text{-}P]^{2-}$	6.5[d]	5.5	
AMP^{2-}	6.2–6.3[e]	5.7	40
ADP^{3-}	6.4–6.5[e]	4.6	4.0
ATP^{4-}	6.5–6.9[d,e]	4.3[f]	4.2

[a] Protonation of the terminal phosphate dianion. [b] Solutions contained 130 mM ligand and 100 mM Mg^{2+}. [c] Literature data for protonation of the adenine ring (N-1) in the absence of added Mg^{2+}.[25,26] [d] From ref 69. [e] Literature data from refs 19, 21, 25, and 26. [f] An additional inflection was observed (Figure 2) that may correspond to protonation of either the α- or γ-phosphate. This was not observed in the $\Delta\nu_{1/2}(^{25}Mg^{2+})$ vs pH profile for ADP^{3-}.

In this case, $k_{on} = K_{os}k_i = K_a k_{off}$, where k_{on} and k_{off} are the on- and off-rates for magnesium binding to the phosphate ligand, respectively, K_{os} is the outer-sphere association constant, k_i is the rate of interchange between the outer and inner coordination shells, and K_a is the association constant for magnesium binding. When a bidentate ligand is used, a second interchange step k_{i2} must be considered, and $k_{on} = K_{os}k_i\,(1 + k_i/k_{i2})^{-1}$.[61] Normally, $k_{i2} > k_i$, and so to a good approximation the correction factor can be neglected. Considering the mono-, di-, and triphosphate ligands in Table I, differences in k_{on} must arise from variations in the values of K_{os} for each complex. Substitution reactions of Mg^{2+} usually involve rate-limiting loss of an inner-sphere H_2O ($k_i \sim 10^5\ s^{-1}$).[26-33] Since $k_{on} = K_{os}k_i$, we estimated the values of K_{os} for each ligand in Table I. For tRNA, it is likely that the large majority of weakly bound ions are held in an outer-sphere coordination mode,[37,48,57] and so we assume $K_{os} = K_a$. These results correlate rather well with the potential for each type of ligand to form H-bond contacts to $Mg(H_2O)_6^{2+}$ (estimated empirically from computer graphics and molecular models). Outer-sphere association constants have been calculated for adenosine phosphates [K_{os} (M^{-1}) = 10, 34, and 80 for AMP^{2-}, ADP^{3-}, and ATP^{4-}, respectively][34] by using the Fuoss equation.[62] This theory is based on considerations of electrostatic attraction and does not implicitly account for other factors (e.g., hydrogen bonding) that might stabilize the outer-sphere complex. As expected, K_{os} also reflects the product of the charges (Z^+Z^-) on the cations and anions, respectively, although in the case of tRNA this would depend on the magnitude of the effective charge at the magnesium-binding site. However, since a substantial portion of the binding energy must derive from H-bonding, it appears reasonable that a correlation between K_{os} and the number of H-bonds should also exist. The numbers of H-bonds in the outer-sphere complexes for the ligands listed in Table I were estimated by using computer graphics and simple molecular models [monophosphates (2 ± 1), ADP^{3-} (3 ± 1), ATP^{4-} (4 ± 1), tRNA (7 ± 2)]. The discrepancy between the calculated values of K_{os} and our experimental data (Table I) may reflect this additional contribution to the binding energy. The distinction is analogous to the difference between ionic and covalent contributions in standard bonding theory. Note that this is distinct from the above discussion concerning the possible relationship between the number of bonding contacts and the exchange regime for a particular ligand. The latter considers the final coordination sphere of the complex, including inner- and outer-sphere components.

Binding Chemistry. There has been much discussion in the literature of the solution structures of $Mg(ATP^{4-})$ and $Mg(ADP^{3-})$ complexes.[28,30,52-54] As discussed above, a large body of evidence supports the specificity of Mg^{2+} binding to the β,γ-phosphate unit of ATP^{4-} and the α,β unit of ADP^{3-},[29,31] The question of whether Mg^{2+} binds directly to the phosphate groups in an inner-sphere mode or via H-bonding from an outer-sphere complex of $Mg(H_2O)_6^{2+}$ has also been discussed.[30,52,54] The magnitude of K_a for ADP^{3-} and ATP^{4-} suggests direct chelation and would argue strongly against the latter possibility. We have described a more definitive test of the composition of the inner coordination shell of Mg^{2+} in a separate paper by determination of the quadrupole coupling constant (χ_B) of the Mg^{2+} nucleus, which reflects the asymmetry (coordination state) of the metal ion.[48] An appreciation of the coordination chemistry for Mg^{2+}–phosphate interactions is of obvious importance in understanding enzymatic mechanisms of metal-dependent phosphate ester hydrolysis, phosphoryl transfer, and phosphatase activity. We shall not discuss in any detail the kinetics or mechanisms of such enzymatic chemistry but offer one example of how the work described in this paper may be relevant to understanding the catalytic chemistry of metal centers in these enzymes. A key observation to note from the discussion above is the influence of Mg^{2+} on the pK of the middle phosphates in polyphosphate anions and also, as a corollary, the effect of protonation in directing Mg^{2+} to the terminal phosphate in contrast to the normal assignment of proton uptake. It is suggested from the data herein that structure V is preferred over IV (Figure 3): divalent magnesium is a harder Lewis acid than H^+ and therefore binds preferentially to the most basic site. Miller and Ukena have shown that diesters of pyrophosphoric acid [$(RO)_2OP\text{–}O\text{–}PO_3^{2-}$] are hydrolyzed ca. 10 times faster than monoesters [$(RO)(O^-)OP\text{–}O\text{–}PO_3^{2-}$] at neutral pH,[63] while metal ions can activate the phosphorylation of phosphate by ATP.[64,65] The possibility of metal ion assistance of nucleophilic attack at the terminal phosphate of ATP has been noted.[13] Bringing these two points together, a possible scenario for the activity of Mg^{2+} would involve (1) activation of the β-phosphate toward protonation by an enzyme residue, generating an activated "diester"–pyrophosphate unit (Figure 3, VI), and (2) relief of electrostatic repulsion between an incoming nucleophile and the terminal dianionic phosphate.[66] Note that the former would not necessarily be favorable in a non-enzyme reaction because the β-phosphate of ATP would not be protonated (Figure 3, VI) at the high pH's required to provide an effective nucleophile (viz., a dianionic phosphate or a carboxylate). This offers further insight and elaboration on proposed mechanisms of kinase activity,[67] for example, and provides a rationale for the absence of significant catalysis by metal ions in non-enzyme hydrolysis of phosphates under physiological conditions.

Summary. We have determined a number of important kinetic and thermodynamic parameters for Mg^{2+} binding to biological substrates by direct analysis of ^{25}Mg NMR line shapes, identified the location of binding sites on polyphosphate anions, and illustrated how metal ion cofactors can influence the relative pK's of neighboring phosphate sites. Relative binding affinities of Mg^{2+} and H^+ for phosphate oxygens are readily understood: Mg^{2+} is a harder Lewis acid and binds to the most basic ligand site. The data support outer-sphere coordination by $Mg(H_2O)_6^{2+}$ to RNA.[68] A detailed knowledge of the coordination chemistry of Mg^{2+} with polyphosphate anions provides an essential basis for understanding the role of divalent metal ions in activating substrates toward enzymatic catalysis. The absence of significant catalysis by metal ions in non-enzyme reactions under physiological conditions is commonly taken as an indicator of specific structural or chemical features peculiar to enzymatic mechanisms. One such interaction may involve metal-activated protonation of phosphate units in a pH range accessible to ionizable protein residues (Figure 3, VI).

Acknowledgment. I thank Susan Reid for atomic absorption measurements, Charles Cottrell for advice on multinuclear NMR

(61) Hammes, G. G.; Steinfield, J. I. *J. Am. Chem. Soc.* **1962**, *84*, 4639.
(62) Levine, S.; Rosenthal, D. In *Chemical Physics of Ionic Solutions*; Conway, B., Barradas, R., Eds.; Wiley: New York, 1966.
(63) Miller, D. L.; Ukena, T. *J. Am. Chem. Soc.* **1969**, *91*, 3050–3053.
(64) Lowenstein, J. M. *Biochem. J.* **1958**, *70*, 222–230.
(65) Lowenstein, J. M.; Schatz, M. N. *J. Biol. Chem.* **1961**, *236*, 305–307.
(66) Walsh, C. *Enzymatic Reaction Mechanisms*; Freeman: New York, 1979; p 181.
(67) Mildvan, A. S.; Cohn, M. *Adv. Enzymol.* **1970**, *33*, 1.
(68) This refers to general magnesium binding and not to the few specialized strong sites noted on tRNA.[57]
(69) Johnson, M. J. In *The Enzymes*; Boyer, P. D., Lardy, H., Kyrback, K., Eds.; Academic: New York, 1960; Vol. 3, Chapter 21.

spectroscopy, and Torbjorn Drakenberg (Lund) for providing data analysis programs. FT-NMR spectra (300 MHz) were obtained at The Ohio State University Chemical Instrument Center. This work was supported in part by a grant from the Elsa U. Pardee Foundation.

Registry No. ADP^{3-}, 58-64-0; 5'-AMP, 61-19-8; 5'-ATP, 56-65-5; Mg, 7439-95-4; glucose 1-phosphate, 59-56-3; glucose 6-phosphate, 56-73-5; acetyl phosphate, 590-54-5.

Contribution from the Department of Physical and Inorganic Chemistry, University of Adelaide, South Australia 5001, Australia

Structural, Equilibrium, and Kinetic Study of the Complexation of Sodium(I) by the Cryptand 4,7,13,16-Tetraoxa-1,10-diazabicyclo[8.8.5]tricosane, $C22C_5$

Philip Clarke, Stephen F. Lincoln,* and Edward R. T. Tiekink

Received October 29, 1990

The cryptate (4,7,13,16-tetraoxa-1,10-diazabicyclo[8.8.5]tricosane)sodium(I) perchlorate, $[Na.C22C_5]ClO_4$, crystallizes in the orthorhombic space group *Pbca* with unit cell dimensions $a = 15.893$ (3) Å, $b = 15.782$ (2) Å, $c = 17.656$ (3) Å, and $V = 4428.5$ Å^3 with $Z = 8$. The structure was refined by a full-matrix least-squares procedure to final $R = 0.045$ and $R_w = 0.054$ for 1669 reflections with $I \geq 2.5\sigma(I)$. The Na^+ center is five-coordinate and lies in the same plane as the four oxygen atoms of $C22C_5$, with the fifth coordination site occupied by a perchlorate oxygen atom above this plane completing a square-pyramidal coordination geometry. An unusual feature is that the two nitrogen atoms of $C22C_5$ (which lie below the plane of the four oxygen atoms) are not within bonding distance of Na^+. This contrasts with the structure of the closely related $[Na.C221]^+$, (4,7,13,16,21-pentaoxa-1,10-diazabicyclo[8.8.5]tricosane)sodium(I), in which Na^+ is in the center of the cryptand cavity and is within bonding distance of all five oxygen atoms and both nitrogen atoms, and illustrates the major structural effect of the replacement of an oxygen donor atom of $[Na.C221]^+$ by a methylene moiety to give $[Na.C22C_5]^+$. This replacement also has a substantial effect in solution where, in acetonitrile, propylene carbonate, water, acetone, methanol, dimethylformamide, dimethyl sulfoxide, and pyridine, log (K/mol dm^{-3}) = ≥7, ≥7, 1.8, 6.09, 5.41, 3.66, 3.15, and 6.41, respectively at 298.2 K, which are substantially smaller values than those characterizing $[Na.C221]^+$. In methanol, the decomplexation kinetic parameters $k_d(298.2\ K) = 41.0 \pm 1.7\ s^{-1}$, $\Delta H_d^* = 55.1 \pm 1.1$ kJ mol^{-1}, and $\Delta S_d^* = -29.2 \pm 3.8$ kJ mol^{-1} characterizing $[Na.C22C_5]^+$ indicate that $[Na.C22C_5]^+$ is several orders of magnitude more labile than $[Na.C221]^+$. These characteristics of $[Na.C22C_5]^+$ are compared with those of related cryptates and are also discussed in terms of the reported greater efficiency of $C22C_5$ as a membrane transport carrier for Na^+ by comparison to C221.

Introduction

The cryptands, or polyoxadiazabicycloalkanes, are substrate specific receptor molecules generated through the current interest in molecular recognition chemistry. A particularly strong correlation between cation size, cryptand cavity size, cryptate structure, and thermodynamic stability is observed for the complexation of alkali-metal ions by cryptands to form cryptates.[1-9] Thus 4,7,13,16,21-pentaoxa-1,10-diazabicyclo[8.8.5]tricosane, C221 (Chart I), with a cavity radius[2] of ca. 1.10 Å, accommodates Na^+ ($r = 1.02$ Å)[10] in the center of the cavity to form *inclusive* $[Na.C221]^+$, but the larger K^+ ($r = 1.38$ Å) is too large to be accommodated, and $[K.C221]^+$ has an *exclusive* structure in which K^+ resides outside the cryptand cavity.[8] These size correlations are reflected in the variation of the stability of $[M.C221]^+$ with M^+ in the sequence $Li^+ < Na^+ > K^+$ in a range of solvents consistent with Li^+ ($r = 0.76$ Å) easily entering the C221 cavity, but being too small to establish optimal bonding distances, and *inclusive* $[Na.C221]^+$ possessing a greater stability than *exclusive* $[K.C221]^+$.[2,3,9]

One of the objectives of molecular recognition studies has been to develop substrate specific carrier molecules for membrane transport, and it is found that the replacement of a cryptand oxygen donor atom with a methylene group generally produces a more effective carrier molecule for transport of alkali-metal ions across membranes.[4] Thus 4,7,13,16-tetraoxa-1,10-diazabicyclo-

Chart I

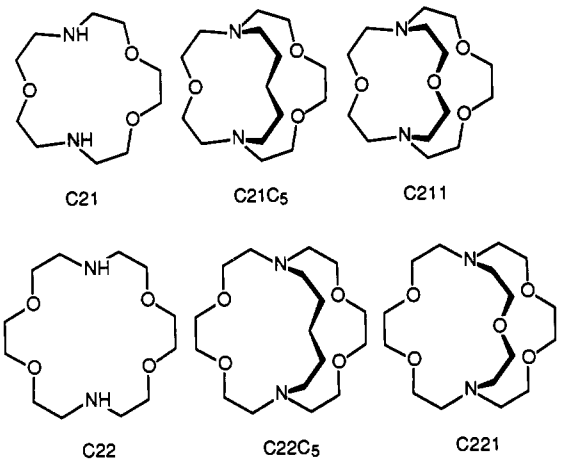

[8.8.5]tricosane, $C22C_5$, is a substantially more efficient carrier for Na^+ than is C221, and $C21C_5$ is a more efficient carrier for Li^+ and Na^+ than is C211. However, there have been only a few systematic studies[11-15] of the effect of the replacement of oxygen donor atoms by methylene moieties on cryptate characteristics. Accordingly a solid-state structural and solution equilibrium study of $[Na.C22C_5]^+$ is reported here, and comparisons are made with $[Na.C221]^+$, $[Na.C22]^+$ (C221 and $C22C_5$ may be viewed as C22 substituted by a $-(CH_2)_2O(CH_2)_2-$ and a $-(CH_2)_5-$ bridge between the two nitrogens, respectively), and other cryptates.

(1) Lehn, J.-M. *Struct. Bonding (Berlin)* **1973**, *16*, 1-69.
(2) Lehn, J.-M.; Sauvage, J. P. *J. Am. Chem. Soc.* **1975**, *97*, 6700-6707.
(3) Lehn, J.-M. *Acc. Chem. Res.* **1978**, *11*, 49-57.
(4) Lehn, J.-M. *Pure Appl. Chem.* **1979**, *51*, 979-997.
(5) Lehn, J.-M. *J. Inclusion Phenom.* **1988**, *6*, 351-396.
(6) Moras, D.; Weiss, R. *Acta Crystallogr., Sect. B: Struct. Crystallogr. Cryst. Chem.* **1973**, *B29*, 400-403.
(7) Lincoln, S. F.; Horn, E.; Snow, M. R.; Hambley, T. W.; Brereton, I. M.; Spotswood, T. M. *J. Chem. Soc., Dalton Trans.* **1986**, 1075-1080.
(8) Mathieu, F.; Metz, B.; Moras, D.; Weiss, R. *J. Am. Chem. Soc.* **1978**, *100*, 4412-4416.
(9) Cox, B. G.; Garcia-Rosa, J.; Schneider, H. *J. Am. Chem. Soc.* **1981**, *103*, 1384-1389.
(10) Shannon, R. D. *Acta Crystallogr., Sect. A: Cryst. Phys. Diffr., Theor. Gen. Crystallog.* **1976**, *A32*, 751-767.
(11) Lincoln, S. F.; Steel, B. J.; Brereton, I. M.; Spotswood, T. M. *Polyhedron* **1986**, *5*, 1597-1600.
(12) Lincoln, S. F.; Brereton, I. M.; Spotswood, T. M. *J. Am. Chem. Soc.* **1986**, *108*, 8134-8138.
(13) Clarke, P.; Abou-Hamdan, A.; Hounslow, A. M.; Lincoln, S. F. *Inorg. Chim. Acta* **1988**, *154*, 83-87.
(14) Abou-Hamdan, A.; Hounslow, A. M.; Lincoln, S. F.; Hambley, T. W. *J. Chem. Soc., Dalton Trans.* **1987**, 489-492.
(15) Lincoln, S. F.; Abou-Hamdan, A. *Inorg. Chem.* **1990**, *29*, 3584-3589.

0020-1669/91/1330-2747$02.50/0